Journal of Cellular Biochemistry Supplement 37:71–81 (2001)

Resonance Light Scattering Particles as Ultrasensitive Labels for Detection of Analytes in a Wide Range of Applications

Juan Yguerabide* and Evangelina E. Yguerabide

Genicon Sciences Corporation, Sorrento Valley Road, San Diego, California

Abstract We have developed a new detection technology that uses resonance light scattering (RLS) particles as labels for analyte detection in a wide range of formats including immuno and DNA probe type of assays in solution, solid phase, cells, and tissues. When a suspension of nano sized gold or silver particles is illuminated with a fine beam of white light, the scattered light has a clear (not cloudy) color that depends on composition and particle size. This scattered light can be used as the signal for ultrasensitive analyte detection. The advantages of gold particles as detection labels are that (a) their light producing power is equivalent to more than 500,000 fluorescein molecules, (b) they can be detected at concentrations as low as 10^{-15} M in suspension by eye and a simple illuminator, (c) they do not photobleach, (d) individual particles can be seen in a simple student microscope with dark field illumination, (e) color of scattered light can be changed by changing particle size or composition for multicolor multiplexing, and (f) they can be conjugated with antibodies, DNA probes, ligands, and protein receptors for specific analyte detection. These advantages allow for ultra-senstive analyte detection with easiness of use and simple and relatively inexpensive instrumentation. We have shown that our RLS technology can indeed be used for ultra-sensitive detection in a wide range of applications including immuno and DNA probe assays in solution and solid phases, detection of cell surface components and in situ hybridization in cells and tissues. Most of the assay formats described in this article can be adapted for drug fast throughput screening. J. Cell. Biochem. Suppl. 37: 71–81, 2001. © 2002 Wiley-Liss, Inc.

Key words: fluorescence labels; ultra-sensitive light scattering labels; ultra-sensitive analyte detection; immunoassays; DNA probe assays; expression microarrays; genotyping microarrays; surface receptor detection; in situ hybridization; immuno-histopathology; viral detection

We have observed that when a suspension of gold particles is illuminated by a narrow beam of white light, the scattered light has a clear (not cloudy) color (see Fig. 1). These observations suggested to us that submicroscopic resonance light scattering (RLS) particles could be used as light scattering labels for ultrasensitive analyte detection in a wide range of applications [Yguerabide and Yguerabide, 1998a,b] including (a) cell biology, (b) histology, and (c) solution and solid phase immuno and DNA probe assays. The advantages of RLS particle labels are: (a) the light scattering power of a 60 nm gold particle is equivalent to about 5×10^5 fluorescein molecules (approximate relative light scattering powers can be inferred from the images and concentrations shown in Figure 1 and its legend), (b) RLS particles do not photobleach, (c) light scattered by RLS particles can be detected by the unaided eye at particle concentrations as low as 10^{-15} M in suspension and as low as 0.005 particles/μ^2 on a transparent surface depending on particle size, (d) individual RLS particles can be seen by eye in an inexpensive student microscope with simple dark field illumination allowing for very sensitive and inexpensive particle counting assays, (e) RLS particles that scatter light of different colors can be obtained by changing particle composition or size (see Fig. 1) and these particles can be used for multicolor multiplexing applications, (f) RLS particles can be coated with specific antibodies, receptors, ligands, or DNA probes for detection of specific analytes and without affecting their light scattering properties, (g) nonspecific binding of RLS particles in solid

*Correspondence to: Juan Yguerabide, 11585 Sorrento Valley Road, San Diego, CA 92121.
E-mail: jyguerabide@geniconsciences.com

Received 17 October 2001; Accepted 22 October 2001

DOI 10.1002/jcb.10077

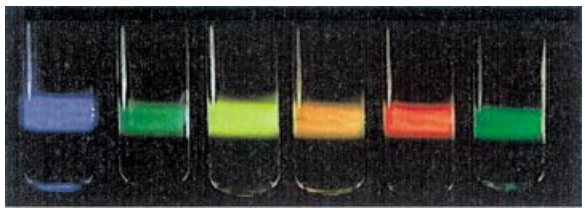

Fig. 1. Photograph showing the appearance of light-scattering suspensions of silver and gold particles and fluorescein when illuminated with a narrow beam of white light. From left to to right: 40 nm silver (2×10^{-12} M), gold, 40 nm (1.3×10^{-11} M), 78 nm (1.7×10^{-11} M), 118 nm (5×10^{-13} M), and 140 nm (3×10^{-13} M). Fluorescein solution (2×10^{-6} M) [Yguerabide and Yguerabide, 1998a].

phase, cell and tissue assays can be reduced to insignificant levels by simple blocking agents, (h) when properly prepared, bare (uncoated) RLS particles can be washed by centrifugation and stored for long time intervals without aggregation or deterioration, (i) when properly prepared, coated RLS particles can be washed and concentrated by centrifugation, passed through chromatographic columns and stored for long time intervals without aggregation, (j) ultrasensitive homogeneous and heterogeneous RLS assays can be performed using relatively simple instrumentation, and (k) ultrasensitive qualitative assays can be performed with eye detection.

In the past few years, we have successfully applied our RLS particle detection technology in a wide of range of analytical formats, including (1) homogeneous assays in the liquid phase, (2) immunoassays in standard microtiter wells, (3) protein and DNA glass and membrane microarrays, (4) electrophoretic blots, (5) in situ hybridization (ISH), (6) immunocytology, (7) immunohistology, and (8) microfluidic studies and assays.

In the following sections, we discuss some of the light scattering properties of RLS particles that are important in their use as light scattering labels and present the results of applications in a variety of formats. Most of the formats discussed in this article can be adapted to fast throughput drug screening.

LIGHT SCATTERING PROPERTIES OF RLS PARTICLES

1. When a particle is illuminated by a beam of monochromatic light, the electric force exerted by the oscillating electric field causes the electrons in the particles to oscillate at the same frequency as the incident light. According to electromagnetic theory, the oscillating electrons emit electromagnetic radiation that has the same frequency (same wavelength) as the incident light. It is this radiation that constitutes the scattered light [Kauzman, 1957; Kerker, 1969; van de Hulst, 1981; Bohren and Huffman, 1983].
2. When a particle suspension is illuminated with monochromatic light of a specific color, the color of scattered light is the same as the incident light and is independent of particle composition or size [Kerker, 1969; van de Hulst, 1981; Bohren and Huffman, 1983; Yguerabide and Yguerabide, 1998a,b]. This property follows from the one above and is one of the features that most distinguishes light scattering from fluorescence. The color of fluorescence produced by a specific substance is independent of the excitation wavelength of exciting light and depends on the composition of the fluorescent molecule. These differences between scattered light and fluorescence must be taken into consideration in the design of procedures and instrumentation for the use of light scattering particles as detection labels.
3. The distinct scattered light colors displayed by particles of different sizes and compositions (as demonstrated in Fig. 1) are only observed with white light illumination (e.g., filament lamp illumination). These distinct colors are due to light scattering spectral bands in the visible region of the spectrum that depend on particle compositions and sizes. When illuminated with white light, a particle suspension preferentially scatters light that has a color that corresponds to the peak wavelength of its light scattering spectral band [Yguerabide and Yguerabide, 1998a,b].
4. In the small particle size range (particle radius a much smaller than the wavelength of incident light), the intensity of light scattered by a particle depends on the sixth power of the radius, a^6 and the light scattering spectrum (as well as color of scattered light with white light illumination) is independent of particle size. The very rapid sixth power increase in scattered light intensity with increase in particle size can be seen experimentally by viewing, for example, a mixture of gold particles of different sizes (less than 40 nm diameter) in the dark field

microscope. All of the particles appear green but display large differences in brightness. These effects can also be seen by illuminating, with white light, gold particles suspensions that have particles of different sizes but same particle concentrations [Yguerabide and Yguerabide, 1998a,b].

5. In the large particle size range (particle size comparable or larger than the wavelength of incident light), increase in particle diameter results in a rapid increase in scattered light intensity, shifts the light scattering spectrum to longer wavelengths and shifts the light scattering color towards the red [Yguerabide and Yguerabide, 1998a,b]. These effects are shown for gold particles greater than 40 nm in Figure 1. The scattered light color shifts to longer wavelengths as the particle diameter is increased.
6. Using the Rayleigh theory of light scattering (which applies in the small particle range), we have calculated the light scattering spectra for particles with many different compositions [Yguerabide and Yguerabide, 1998a,b]. The spectra for a selected number of compositions are shown in Figure 2. For most compositions, the scattered light intensity decreases continuously with increasing wavelength. These compositions scatter blue light when illuminated with white light. Silver and gold particles display light scattering bands at 380 and 520 nm and, respectively, scatter purple and green light. Compositions that display light scattering bands and have high light scattering powers are preferred for RLS labels. The light scattering spectra of Figure 2 are normalized and do not give any information on the relative light scattering powers of the different compositions. Table I shows the light scattering powers of particles of different compositions in terms of light scattering cross sections. Column 3 lists relative light scattering powers in a scale where silver particles are assigned a value of 1000. The latter column shows that gold and silver particles have the highest light scattering powers. Columns 4 and 5 show light scattering powers expressed in terms of molar decadic extinction coefficients ε and fluorescence efficiencies φ. Relative light scattering power is related to the product εφ. It can be seen

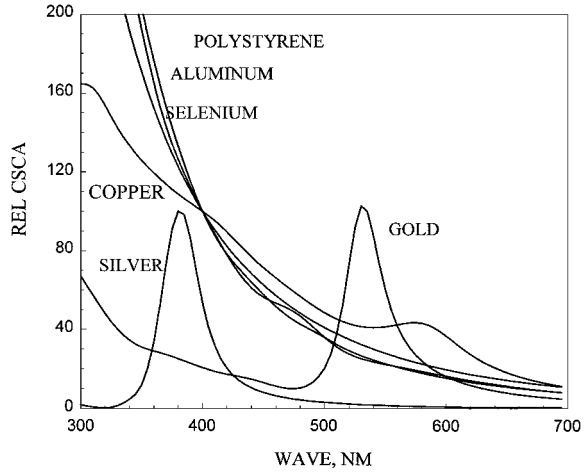

Fig. 2. Graphs of relative light-scattering cross section vs. wavelength for small particles (Rayleigh limit) of different compositions. The graphs for gold and silver have been normalized so that their peak values are 100. The other graphs which do not show a maxima above 380 nm are normalized so that their normalized scattering cross sections have a value of 100 at 400 nm [Yguerabide and Yguerabide, 1998a].

TABLE I. Calculated Light Scattering and Absorption Properties for Particles of Different Compositions (Rayleigh Scattering)

	CSCA (cm^2)	WAVE (nm)	REL CSCA	ε (M^{-1} cm^{-1})	φ_s
Silver	8×10^{-12}	380	1000	1.68×10^{10}	0.126
Gold	9.02×10^{-13}	530	112.7	5.88×10^{9}	0.04
Copper[a]	3.74×10^{-13}	380	46.8	2.59×10^{9}	0.038
	1.43×10^{-13}	530	17.9	1.53×10^{9}	0.025
Aluminum[a]	3.73×10^{-13}	380	46.6	2.66×10^{8}	0.369
	7.49×10^{-14}	530	9.36	8.77×10^{7}	0.225
Selenium[a]	1.85×10^{-13}	380	23.1	5.41×10^{8}	0.09
	3.69×10^{-14}	530	4.61	1.69×10^{8}	0.057
Polystyrene[a]	3.76×10^{-15}	380	0.47	9.88×10^{5}	1
	9.93×10^{-16}	530	0.124	2.61×10^{5}	1

Values given in the table were calculated with the Rayleigh equation. Particle diameter = 30 nm. Medium refractive index = 1.33. Wave = wavelength; Rel Csca = scattering cross section divided by scattering cross section of silver at 380 nm and multiplied by 1000. ε = Molar decadic extinction coefficient; φ_s = Light scattering yield.

[a]This particle does not have a prominent light scattering or absorption peak in the visible region of the spectrum. The cross sections decrease continuously with increasing wavelength. Data are arbitrarily tabulated at the wavelengths shown in the table.

that the high light scattering powers of silver and gold are due to their very high values of ε which are around 10^{10} M^{-1} cm^{-1} compared, for example, to an ε value of 6×10^4 for fluorescein. For larger diameter gold particles, the values of ε ($cm^{-1}M^{-1}$) and φ are: 40 nm (1.63×10^{10}, 0.1), 60 nm (5.32×10^{10}, 0.31), 80 nm (1.14×10^{11}, 0.546), 100 nm (1.62×10^{11}, 0.739). The bandwidth (full width at half maximum) of the light scattering band for 40 nm diameter gold particles is around 20 nm and increases to about 50 nm for 80 nm diameter particles.

7. It is well known that a particle composed of a transparent dielectric material (such as polystyrene, silica, or polyacrylamide) does not scatter light and is invisible when bathed by a medium (solvent) that has the same refractive index as the particle [Yguerabide and Yguerabide, 1998a,b]. More specifically, the scattered light intensity (monochromatic illumination) of a particle goes through a minimum with zero value when the refractive index of the medium (nmed) is increased starting from a value of nmed = 1 (air). On the other hand, the scattered light intensity of gold and silver particles increases continuously (does not go through a minimum) with increase in refractive index starting from nmed = 1. The particles become very bright and their scattered light color (white light illumination) shifts to the red as the medium refractive index is increased. We use these different effects of nmed on particles composed of dielectric materials and silver and gold to reduce background scattering in some RLS assays, for example, filter membrane assays, as discussed below.
8. The relation between scattered light intensity, Is and particle concentration, c has been characterized experimentally (Yguerabide and Yguerabide, unpublished communications). Scattered light intensity increases continuously with increase in particle concentration and reaches a saturation value at high particle concentrations. The scattered light intensity is proportional to the amount of incident light that is absorbed by the particle suspension (which obeys the Beer-Lambert law for light absorption) and saturation of the intensity signal occurs at concentration where all of the incident light is absorbed. The dynamic range for detection of scattered light intensity is about three decades. The detection limit for 80 nm gold particles is around 5×10^{-15} M in particle concentration. The detection limit decreases (sensitivity increases) with increase in particle size. Similar relations describe Is vs. particle surface density in solid phase assays.

INSTRUMENTATION FOR RLS DETECTION

As already stated, the very high light producing power of RLS particles allows ultrasensitive assays to be conducted using relatively simple instrumentation. For RLS applications in cell biology, histology, microarrays, and microfluidics, we use a simple student microscope modified for dark light illumination with a 100 W filament lamp. The light from the lamp is conducted to the microscope stage by a flexible light guide and focused on the sample with a lens. To produce dark background illumination, the light guide and focusing lens are angled with respect to the microscope objective so that the illuminating light does not directly enter the objective. This method of illumination is less expensive and more efficient than the dark field illuminators used in conventional dark field microscopes [Yguerabide and Yguerabide, 1998a,b]. Our microscope arrangement allows simultaneous examination of cells and tissue preparations by dark field as well as low level bright field illumination using a combination of RLS particles and conventional histological dyes. Images can be recorded with a photographic, video, or digital camera. The field of view of a microscope is at most a few millimeters with a low magnification objective. For microarrays that consists of thousands of spots spread over a whole microscope slide, the microscope allows detection of only a few spots at a time. For a wider field of view, we use in place of the microscope, a video or digital camera with a video lens that has the appropriate field of view. However, if high spatial resolution is important, then the lens magnification must be adjusted so that the number of pixels per unit image area is consistent with the desired spatial resolution. If the detected area is smaller than the total sample area, then different sample areas must be separately recorded and then stitched together to form an image of the whole array or sample. We have found that RLS labeled microarrays can also be imaged using the standard scanners or CCD camera instruments commonly used to quantify fluorescence labeled DNA arrays.

For detection of light scattering intensity from particle suspensions, as for example, in liquid phase RLS homogeneous assays, we use a fine beam of white light to illuminate the suspension and a photodiode for light detection. To minimize stray light detection, we use lenses and apertures to isolate light scattered by the RLS particle from light reflected and scattered by the walls of the container.

We have also constructed instruments for measuring corrected light scattering spectra from particle in suspensions and on solid surfaces. These measurements are very helpful in the development of RLS multicolor applications.

CONJUGATION OF PROTEINS, DNA PROBES, AND LIGANDS TO RLS PARTICLES

To detect specific analyte molecules with RLS particles, it is necessary to coat or conjugate the particles with substances that bind selectively to specific analytes. It is well known that gold particles can easily be conjugated with specific proteins by simply adding the protein to a gold particle suspension [Faulk and Taylor, 1971; Geoghegan and Ackerman, 1977; Goodman et al., 1979; Horisberger, 1981; Horisberger and Clerc, 1985]. The protein molecules spontaneously bind noncovalently to the gold particles. We use this procedure to bind specific antibodies to RLS particles for RLS immunoassays. However, DNA probes or low molecular weight ligands do not bind spontaneous to RLS particles. To bind the latter types of substances, we first coat the particles with polymers that have reactive groups such amine or carboxyl groups. We then use the reactive groups to covalently bind DNA or ligands to the particles. Bifunctional reagents with one sulhydryl group and one carboxyl or amine group can also be used for covalent conjugation to gold particles, making use of the fact that sulfhydryl groups strongly bind to gold particles [Shigekawa and Hsieh, 1995; Chen and Kimura, 1999].

To the minimize the amount of chemistry needed to prepare RLS particles for detecting specific DNA sequences and antigens, we use procedures that allow us to conduct a wide range of assays using only three or four different antibodies conjugated to RLS particles. Most of the popular DNA microarray methods require PCR amplification or reverse transcriptase synthesis of target DNA. During this amplification or synthesis, biotin can be incorporated into the target DNA. Detection of DNA microarrays can then be conducted with RLS particles conjugated with antibiotin antibodies. Similarly, in solid phase sandwich immunoassays, the second antibody can be labeled with biotin and detection conducted with RLS particles conjugated with antibiotin. Alternatively, we can use RLS particles conjugated with antimouse or antigoat antibodies since most second antibodies are of mouse or goat origin. For DNA microarrays detected by fluorescence, the target DNA is labeled with fluorescein, Cy3 or Cy5. We have been able to compare fluorophore and RLS labeled microarrays by using an intermediate biotinylated antifluorphore antibody. These comparisons are described in the applications section.

APPLICATIONS

Model DNA Probe Test Arrays

To determine the detection dynamic range and sensitivity of our RLS detection technology using RLS particles of different compositions and sizes, we use a relatively simple model system consisting of pdT_{35}-3′ NH_2 as DNA probe immoblized on a glass slide and pdA_{35}-3′-Biotin as target analyte. In this application, the pdT_{35}-3′-NH_2 is immobilized on a glass slide in an array of spots with diameters of 2–3 mm (hand spotting) or 250 μ (robotic spotting). Each spot is hybridized with a different concentration of pdA_{35}-3′-Biotin (less than 1 μl volume per spot) and reacted with gold-antibiotin IgG conjugate. The results show that our RLS detection technology has (1) a three decade dynamic range for detection of pdA_{35}-3′-Biotin concentration and (2) detection sensitivity of around 0.02 immobilized pdA_{35}-3′-Biotin molecules/μ^2.

In another model system, we deposit different amounts of biotinilated PCR DNA product molecules in 250 μ spots and measure the integrated scattered light intensity of each spot. Detection sensitivity in this model system is 1300 PCR product molecules per spot (0.03 molecules/μ^2) with a signal to background ratio of 2. Dynamic detetion range is three decades of PCR product concentration.

Solid Phase DNA and RNA Assays: Gene Expression and Gene Typing Microarray Chips

Solid phase DNA probe assays are based on the original observation [Gillespie and

Spiegelman, 1965] that single stranded DNA binds strongly to nitrocellulose membranes and can hybridize to complementary RNA in this immobilized state. These observations were followed by the development of (a) filter based methods for screening of clones to identify clones with specific DNA sequences, colony hybridization assays [Grunstein and Hogness, 1975], (b) blotting methods for detection of specific DNA or RNA sequences separated by gel electrophoresis [Southern, 1975; Alwine et al., 1977], (c) dot blots for detection of specific analyte DNA sequences [Kafatos et al., 1979], and (d) DNA expression [Schena et al., 1995; De Risi et al., 1997], and (e) DNA variation (mutation, polymorphism) microarrays [Drmanac et al., 1989; Khrapko et al., 1989; Fodor et al., 1991; Pease et al., 1994]. Dot blots and DNA microarrays consists of DNA probe spots (features) each of which contains a different immoblized DNA probe to detect a complementary analyte target sequence in solution. The difference between these two types of arrays is that dot blot arrays are prepared on a porous membranes, whereas, the former are prepared on a nonporous substrate such as glass. The use of glass as substrate permits the deposition of smaller spots (greater number of spots per unit area) and detection with fluorescent labels. We have found that our RLS detection technology can be applied to all of the solid phase DNA formats described above and have definite advantageous in detection sensitivity and easiness of use. Below we review our results for some of these applications.

The two most popular types of DNA microarrays at the present time are the gene expression (cDNA) arrays and the DNA variation microarrays. The expression arrays are designed to detect the levels of expression (abundance of transcripts) of different genes in a defined cell type in different states (e.g., normal and diseased states) by measurement of the amount of mRNA for each of the genes of interest. The immobilized or capture probe sequences are usually cDNA molecules with 0.6–1.2 kb lengths, although 25 mer capture probes are used in high density microarrays [Lockhart et al., 1996]. The cDNA capture probes are obtained from commercially available cDNA clones and amplified by PCR (cDNA expression microarray). The analyte sample is obtained by extracting total RNA or mRNA from a cell sample and converting it to fluorescent or biotin labled cDNA using reverse transcriptase. Abundance level is determined from fluorescence intensity or amount of biotin on each array spot. The DNA variation microarrays are designed to detect gene mutations, especially single nucleotide polymorphisms (SNPs) and use oligonucleotide of about 25 nucleotide as probes immobilized on a glass substrate.

We have tested the ability of our RLS gold particles to serve as detection labels in a variety of expression and DNA variation microarrays, some of which are available commercially. Figure 3a shows images of a gold particle labeled Affymetrix 4N tile SNP (single nucleotide polymorphism) microarray [Pease et al., 1994] for detection of SNPs in the human immunodeficiency virus. The chip has immobilized probes specific for the protease and reverse transcriptase sections of HIV viral RNA. The chip was hybridized with PCR product amplified from a plasmid (50–100 bp DNA fragments) and end labeled with biotin. The hybridize chip was treated with a 80 nm gold-antibiotin IgG particle suspension and washed. Because of the very intense gold scattered light signals, the RLS labeled tiles in the array can be seen by eye using a simple illuminator and magnifying lens. Figure 3a shows the microarray at two different magnifications. The intensity range is more than two decades. Some of the tiles are saturated in intensity because of the limited intensity range of the video camera and printer. The edges of the tiles are sharp and well defined. The low magnification image on the left hand side has a similar appearance to the image seen by eye and a hand held magnifying lens. The sequence of the target nucleotide can be read by eye from the gold-labeled image viewed in the dark field microscope without the need for intensity amplification or image recording.

Figures 3b shows images of a Phase-1 Rat Toxin expression microarray labeled with 80 nm gold antibiotin IgG conjugate particles (right hand image) and the fluorophore Cy3 (left hand image). This array is designed to study drug toxicity effects and includes immobilized sequences that detect the level of expression of genes thought to be involved in toxicity response pathways including those involved in inflammation, detoxification metabolism, apoptosis, cell signaling, oxidative stress, DNA repair, and cell proliferation. The array was

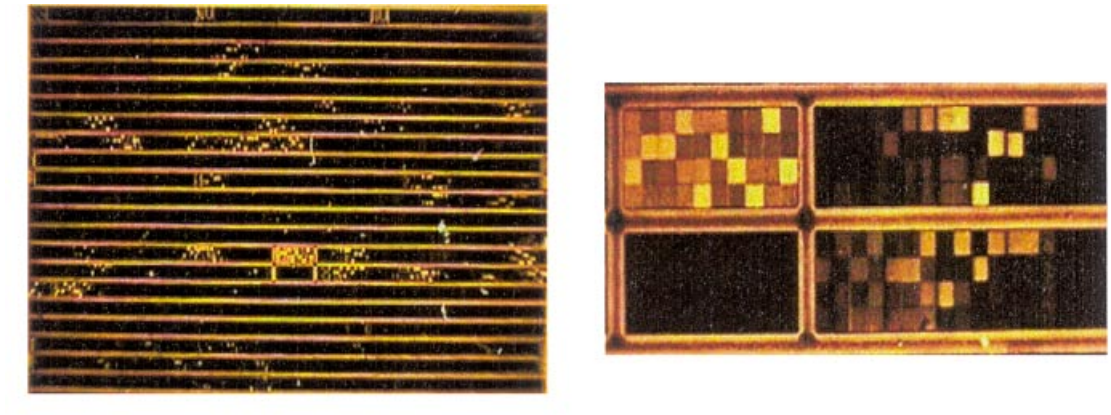

a

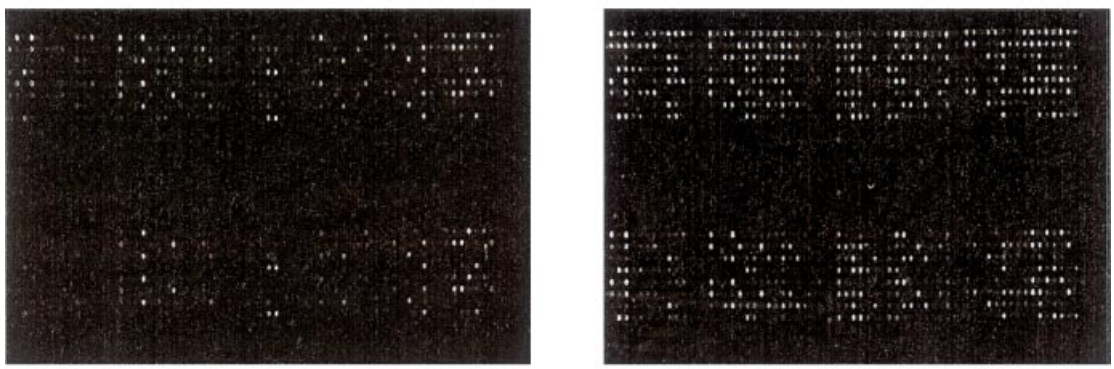

b

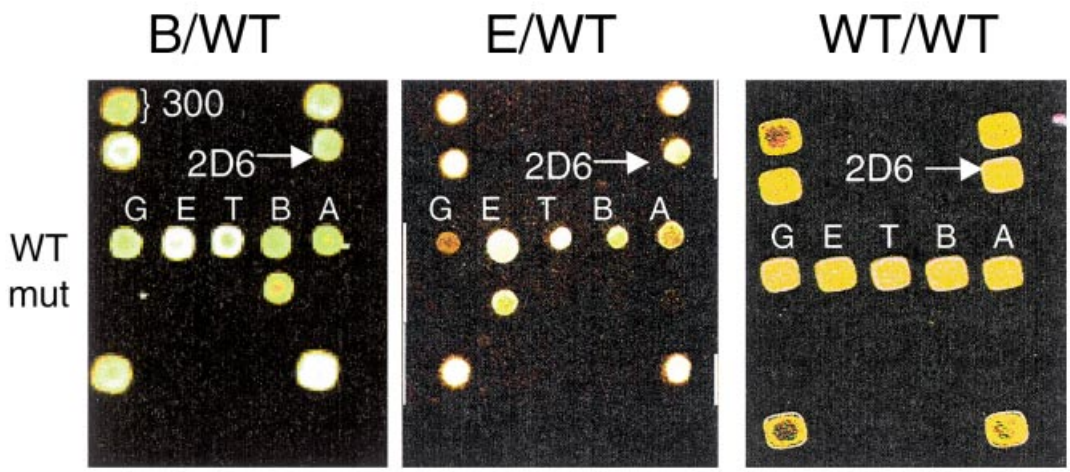

c

Fig. 3. **a**: Images, at two different magnifications, of a gold particle (80 nm) labeled high density array designed for detection of HIV SNPs. **b**: Images of Phase-1 Tox Rat Microarray designed for study of toxic effects of medicinal drugs at the level of gene expression. CDNA from 1 μg of liver poly A^+ RNA was used as analyte target. Left image is detected by fluorescence,CY3 label, (1 s Array WoRx exposure) and right image is detected by 80 nm RLS particles (0.1 s Array WoRx exposure). **c**: Images of a genotyping array designed to detect the wild and A, B, E, G, and T mutant alleles of the CYP2D6 gene. Detection is with 80 nm gold antibiotin IgG conjugates. The rows labeled WT and mut show the spots that detect the wild and mutant alleles. The three images are for three different individuals. Left: heterozygous B/WT, Middle: heterozygous E/WT, Right: homozygous WT/WT.

hybridized with a rat liver cDNA (500–1,000 bp) sample obtained by reverse transcription of a commercial sample of rat liver PolyA$^+$ mRNA. The cDNA had about 5 biotin or Cy3 labels per 1,000 bp. Images of the fluorescent and gold labeled arrays were recorded with an Array WoRx microarray scanner that uses a white light source for illumination and a CCD camera for image detection. Appropriate excitation and barrier filters are used for recording the fluorescence image. The fluorescence and gold particle images were recorded respectively with 1 and 0.1 s integrating times. The results show that the gold particle images are brighter and display more positive features than the Cy3 image (577 vs. 116 positive features). The relative expression level of each gene represented in the array can be determined from the scattered light intensities compared to a reference cDNA sample.

Figure 3c shows images of an array designed at Genicon Sciences for human CYP2D6 genotyping. CYP2D6 is the gene that codes for the liver enzyme cytochrome P450 CYP2D6, which is involved in the metabolism (elimination) of many medicinal drugs. Several alleles of this gene are present in the human population and some of these alleles produce inactive P450 enzyme [Kimura et al., 1989; Heim and Meyer, 1990; Chen, 1996] or no enzyme at all. Persons with defective alleles display drug side effects. The Genicon Sciences CYP2D6 allele detection array shown in Figure 3e is designed to detect the A, B, E, G, and T CYP2D6 alleles. The array consists of five spots for measuring the presence of the wild type (WT) alleles and five spots for detection of the mutated alleles. Two of the arrays shown in the figure are for heterozygous individuals with B/WT and E/WT alleles and one is for an individual that is homozygous for the WT allele. The Genicon CYP2D6 genotyping array has been validated against the standard but tedious method that uses allele specific polymerase chain reaction (PCR) in combination with electrophoretic anlysis of the PCR [Heim and Meyer, 1990; Chen, 1996].

We have compared the sensitivity of RLS detection with ^{32}P detection using a CYP2D6 specific oligonucleotide conjugated with biotin and ^{32}P (5′-^{32}P and 3′-Biotin). Serial dilutions of the oligonucleotide were spotted on aminated glass slides. One slide was used for radioactive and the other for RLS detection. Radioactivity on each spot was measured with a phosphorimager (2.5 days exposure) and the RLS intensity of each spot was detected by with a digital camera (a few seconds exposure). The results indicate that the sensitivity of the RLS method is equivalent to or better than radioactivity but much faster.

Immunowell Assays

As an example, we present our results for detection of *C. difficile* Toxin A by a solid phase sandwich immunoassay. Toxin A causes dysentery and is detected clinically in stool specimens using an ELISA sandwich assay [Ehrich et al., 1980; Lyerly et al., 1983] Using the same antibodies that are used in the commercial ELISA assay (Meridian Diagnostics, Inc., Cincinnati, Ohio), but labeling the second (detection) antibody with biotin instead of enzyme, we determined the sensitivity for RLS particle detection of Toxin A in a pure Toxin A solution and in patient excrement samples. In pure Toxin A solution, we obtain a sensitivity for RLS detection (60 nm gold particles) of about 10^{-14} M Toxin A concentration in a volume of 100 μl with about 1 h incubation time. Higher sensitivity is obtained with longer incubation times. In twenty patient excrement samples (ten positive and ten negative samples as determined by the ELISA method), RLS measurements showed 8 positive and 12 negatives. Ten of the RLS negatives agreed with the 10 ELISA negatives and eight of the RLS positives agreed with 8 ELISA positives. However, two of the RLS negatives tested positive by ELISA. Retesting of the latter by ELISA showed that one of the samples was indeed negative and the other was ambiguous.

Fibrous Membrane Blotting and Dot Blot Arrays

RLS particles cannot be detected with high sensitivity in a dry or water wet membrane because of the very high light scattering background produced by the membrane itself. However, we have found that the intensity of light scattered by the membrane can be considerably reduced by refractive index matching, making use of the differential effects of the bathing medium refractive index on dielectric and metal particles or fibers as described above. In the appropriate index matching bathing medium, the membrane appears as translucent as glass. With index matching we have been able to achieve RLS sensitivities for analyte detection

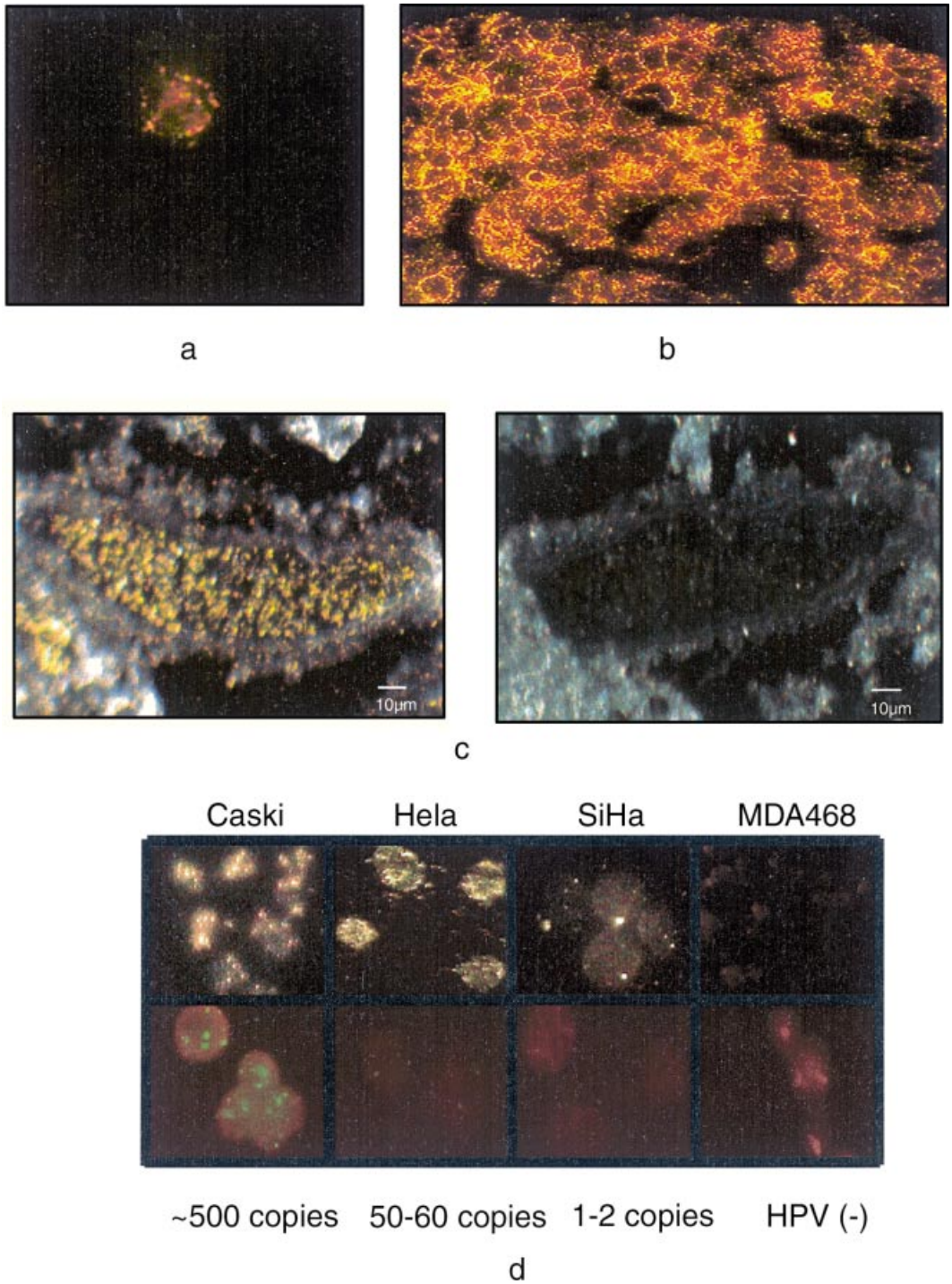

Fig. 4. **a**: Image of human CD4 white blood cell that has been reacted with 60 nm gold antiCD4 IgG conjugate particles. The gold particles bound to the cell surface have been patched and are being drawn into a cap. **b**: RLS immunohistological detection of a cancer antigen. Image of breast carcinoma tissue that has been reacted with mouse HER-2/neu tyrosine kinase antibodies, washed, blocked, and then sequentially treated with biotinylated antimouse antibody and 80 nm gold-antibiotin IgG. The kinase is a plasma membrane bound protein. **c**: RLS detection of a specific gene using ISH. Breast carcinoma tissue was reacted (hybridized) with digoxigenin labeled HER-2/neu specific DNA probe (about 200 kb), washed, treated with biotinylated anti-digoxigenin antibody, washed, blocked, and finally reacted with 80 nm gold-antibiotin IgG conjugatge particles. The figure shows a patch of cells in the breast carcinoma tissue where the HER-2/neu gene is labeled with RLS particles. The negative control was obtained by omitting the biotinylated antibody in the detection procedure. **d**: RLS detection of intracellular viruses by ISH. The amount of HPV in different cell type infected with different amounts of HPV was detected as follows. Commercially available glass slides containing fixed interface nuclei from HPV infected cells were hybridized in situ with the HPV specific DNA probe labeled with fluorescein. The cells were then washed and reacted with 80 nm gold antifluorescein IgG conjugate particles. The labeled cells were detected both by fluorescence (no gold particle labeling) and by 80 nm gold antbiotin IgG particles. Only nuclei with more than about 100 copies of HPV DNA could be detected by fluorescence. One to two copies of HPV DNA could be detected by RLS labeling.

in membrane blotting and dot blot arrays that are better that enzymatic detection and only about 2–4 times lower than RLS sensitivity using a glass substrate.

Cellular and Histological Applications

Figure 4a shows a CD4 lymphocyte cell that has been reacted with 60-nm gold-antiCD4 IgG conjugate particles. The ability to detect individual gold particles by eye in the dark field microscope allowed us observe the interaction dynamics of gold particles with the lymphocyte cell. Human lymphocytes were isolated by Ficoll floatation, mixed with gold-antiCD4 particles and immediately viewed in our dark field microscope. The gold particles were seen to collide and bounce off most of the lymphocytes, but occasionally they became tethered to a lymphocyte, supposedly a CD4 positive cell. The tethered particles wiggle for a few seconds and then become completely immobilized on the cell surface. The bound gold particles then aggregated into patches, migrated towards a cap and the cap was endocytosed.

Figure 4b presents an example of RLS detection of gene protein product using methods of immunohistology. We detected the HER-2/neu gene product tyrosine kinase (transmembrane glycoprotein) in breast carcinoma tissue. HER-2/neu is a proto-oncogene and the human analog of the rat neu gene associated with rat neuroblastoma [Press et al., 1997; Ross and Fletcher, 1999]. Over expression of this gene indicates poor prognosis for breast cancer patients. Thin-sectioned breast carcinoma tissue was sequentially reacted with mouse anti-HER-2/neu tyrosine kinase, biotinylated antimouse antibody and 80 nm gold-antibiotin IgG conjugate. The image of Figure 4b shows that the tissue is intensely labeled with RLS particles and that the particles are chiefly on the cell surface membranes where the HER-2/neu tyrosine kinase is located.

Figure 4c presents an example of RLS detection of a specific gene using ISH. We detected the HER-2/neu gene in breast carcinoma tissue by ISH. Digoxigenin labeled ISH probe (about 200 kb) from Zymed was hybridized to formalin fixed paraffin embedded breast carcinoma tissue. The tissue was then washed, and reacted sequentially with biotinylated antidioxigenin antibody and 80 nm gold-antibiotin IgG. Figure 4c shows a patch of cells in a breast carcinoma tissue where the HER-2/neu is labeled with RLS particles. The negative control was obtained by omitting the biotinylated antidigoxigenin antibody in the detection procedure.

Figure 4d presents examples of RLS detection of viruses in cells using ISH. We detected human papilloma virus (HPV) in infected cells with an HPV specific DNA probe labeled with FITC (fluorescein isothiocyanate). Fixed interface nuclei from HPV infected cells were hybridized in situ with the HPV specific DNA probe. The cells were then washed and blocked and reacted sequentially with mouse antifluorescein antibody, biotinylated antimouse antibody, and 80 nm gold-antibiotin IgG. The labeled cells were detected both by fluorescence (no gold particle labeling) and by 80 nm gold antbiotin IgG particles. As shown in Figure 4d, only nuclei with more than about 100 copies of HPV DNA could be detected by fluorescence. On the other hand, cells with 1–2 copies of HPV DNA could be detected by RLS labeling.

Others have more recently tested the RLS detection technology in certain biological applications [Schultz et al., 2000].

ACKNOWLEDGMENTS

We thank Dr. Todd Peterson, Linda Korb, and Gary Bee for some of the images in Figures 3 and 4 and Khalid Yamout for preparation of the gold-IgG particle conjugates.

REFERENCES

Alwine JC, Kemp DJ, Stark GR. 1977. Method for detection of specific RNAs in agarose gels by transfer to diazobenzyloxymethyl-paper and hybridization with DNA probes. Proc Natl Acad Sci U S A 74:5350–5354.

Bohren CF, Huffman DR. 1983. Absorption and scattering of light by small particles. New York: Wiley.

Chen S, Chou W, Blouin RA, Mao A, Humphries LL, Meek QC, Neill JR, Martin WL, Hays LR, Wedlund PJ. 1996. The cytochrome P450 2D6 (CYP2D6) enzyme polymorphism: Screening costs and influence on clinical outcomes in psychiatry. Clin Pharmacol Ther 60:522–534.

Chen S, Kimura K. 1999. Sunthesis and characterization of carboxylate-modified gold nanoparticle powders dispersible in water. Langmuir 15:1075–1082.

De Risi JL, Lyer VR, Brown PO. 1997. Exploring the metabolic and genetic control of gene expression on a genomic scale. Science 278:680–686.

Drmanac R, Labat I, Brukner I, Crkvenjakov R. 1989. Sequencing of megabase plus DNA by hybridization: theory of the method. Genomics 4:114–128.

Ehrich M, Van Tassell RL, Libby JM, Wilkins TD. 1980. Productin of *Clostridium difficile* antitoxin. Infect Immun 28:1041–1043.

Faulk WP, Taylor GM. 1971. An immunocolloid method for the electron microscope. Immunochemistry 8:1081–1083.

Fodor SPA, Read JL, Pirrung MC, Stryer L, Lu AT, Solas D. 1991. Light-directed, spatially addressable parallel chemical synthesis. Science 251:767–773.

Geoghegan WD, Ackerman GA. 1977. Adsorption of horseradish peroxidase, ovomucoid and anti-immunoglobulin to colloidal gold for the indirect detection of concanavalin A, wheat germ agglutinin and goat anti-human immunoglobulin G on cell surfaces at the electron microscope level: a new method, theory and application. J Histochem Cytochem 25:1187–1200.

Gillespie D, Spiegelman SA. 1965. A qunatitative assay for DNA–RNA hybrids with DNA immobilized on a membrane. J Mol Biol 12:829–842.

Goodman SL, Hodges GM, Trejdosiewiczk LK, Livingston DC. 1979. Colloidal gold probes—a further examination. Scanning Electron Micros 3:619–628.

Grunstein M, Hogness DS. 1975. Colony hybridization: A method for the isolation of cloned DNAs that contain a specific gene. Proc Natl Acad Sci U S A 72:3961–3965.

Heim M, Meyer UA. 1990. Genotyping of poor metabolisers of degrisoquine by allele-specific PCR amplification. The Lancet 336:529–532.

Horisberger M. 1981. Colloidal gold: a cytochemical marker for light and fluorescent microscopy and for transmission and scanning electron microscopy. Scanning Electron Micros 2:9–31.

Horisberger M, Clerc MF. 1985. Labeling colloidal gold with protein A. A quantitative study. Histochemistry 82: 219–223.

Kafatos FC, Jones CW, Efstratiadis A. 1979. Determination of nucleic acid sequence homologies and relative concentrations by a dot hybridization procedure. Nucleic Acids Res 24:1541–1552.

Kauzman W. 1957. Quantum chemistry. New York: Academic Press.

Kerker M. 1969. The scattering of light and other electromagneitic radiation, New York: Academic Press.

Khrapko KR, Lysov YP, Khorlin AA, Shick VV, Florentiev VL, Mirzabekov AD. 1989. An oligonucleotide hybridization approach to DNA sequencing. FEBS Lett 256:118–122.

Kimura S, Umeno M, Skoda RC, Meyer UA, Gonzalez FJ. 1989. The human debrisoquine 4-hydroxylase (CYP2D) locus: Sequence and isdentification of the polymorphic CYP2D6 gene, a related gene, and a pseudogene. Am J Hum Genet 45:889–904.

Lockhart DJ, Deng H, Byrne MC, Follettie MT, Gallo MV, Chee MS, Mittmann M, Wang C, Kobayashi M, Horton H, Brown EL. 1996. Expression monitoring by hybridization to high-density oligonucleotide arrays. Nat Biotechnol 14:1675–1680.

Lyerly DM, Sullivan NM, Wilkins TD. 1983. Enzyme-linked immunosorbent assay for *Clostridium difficile* toxin A. J Clin Microbiol 17:72–78.

Pease AC, Solas D, Sullivan EJ, Cronin MT, Christopher PH, Fodor STA. 1994. Light-generated oligonucloeotide arrays for rapid DNA sequence analysis. Proc Natl Acad Sci U S A 91:5022–5026.

Press MF, Bernstein L, Thomas PA, Meisner LF, Zhou JY, Ma Y, Hung G, Robinson RA, Harris C, El-Naggar A, Slamon DJ, Phillips RN, Ross JS, Wolman SR, Flom KJ. 1997. HER-2/neu gene amplification characterized by fluorescence in situ hybridization: poor prognosis in node-negative breast carcinimas. J Clin Oncol 15:2894–2904.

Ross JS, Fletcher JA. 1999. HER-2/neu (c-erB-2) gene and protein in breast cancer. Am J Clin Pathol 112 (Suppl): S53–S67.

Schena M, Shalon D, Davis RW, Brown PO. 1995. Quantitative monitoring of gene expression patterns with a complementary DNA microarray. Science 270: 467–470.

Schultz S, Smith DR, Mock JJ, Schultz DA. 2000. Single-target molecule detection with nonbleaching multicolor optical immunolabels. Proc Natl Acad Sci U S A 97:996–1001.

Shigekawa BL, Hsieh Y. 1995. Ligand Gold Bonding, US Patent 5,384,073.

Yguerabide J, Yguerabide EE. 1998a. Light scattering submicroscopic particles as highly fluorescent analogs and their use as tracer labels in clinical and biological applications, I. Theory. Anal Biochem 262:137–156.

Yguerabide J, Yguerabide EE. 1998b. Light scattering submicroscopic particles as highly fluorescent analogs and their use as tracer labels in clinical and biological applications, II. Experimental characterization. Anal Biochem 262:157–175.